Hindawi
Mathematical Problems in Engineering
Volume 2019, Article ID 4128438, 12 pages
https://doi.org/10.1155/2019/4128438

Research Article

Target Signal Extraction Method Based on Enhanced ICA with Reference

Liuyang Gao,[1,2] **Nae Zheng**,[1] **Yinghua Tian**,[1] **and Jingzhi Zhang**[1]

[1]*Information Engineering University (IEU), Science Avenue, Zhengzhou 450001, China*
[2]*Luoyang Electronic Equipment Testing Center (LEETC), P.O. Box 061, Luoyang 471000, China*

Correspondence should be addressed to Nae Zheng; 13837122426@163.com

Received 11 May 2019; Revised 14 July 2019; Accepted 7 August 2019; Published 21 August 2019

Academic Editor: Paolo Crippa

Target signal extraction has a great potential for applications. To solve the problem of error extraction of target signals in the current constrained independent component analysis (cICA) method, an enhanced independent component analysis with reference (EICA-R) method is proposed. The new algorithm establishes a unified cost function, which combines the negative entropy contrast function and the distance metric function. The EICA-R method transforms the constrained optimization problem into unconstrained optimization problem to overcome the problem of threshold setting of distance metric function in constrained optimization problem. The theoretical analysis and simulation experiment show that the proposed EICA-R algorithm overcomes the problem of the error extraction of the existing algorithm and improves the reliability of the target signal extraction.

1. Introduction

Target signal extraction is used to extract unknown source signals from multiple linear mixed signals, which has found a wide range of applications. Especially in the case of the complex electromagnetic environment, a substantial number of electromagnetic signals are interwoven together to interfere with each other [1]. When target signals are mixed with interference signals, multiple mixed signals are generated. These mixed signals that overlap and interconnect in the time domain and frequency domain lead to the communication failure. How to extract the target signal effectively from the mixed signals has become one of the hotspots and key points in the field of signal processing [2].

A current trend in target signal separation is the independent component analysis (ICA) approach, the core idea of which is to minimize the statistical relationship between all the signal sources [3, 4]. ICA can effectively separate all the signals, including target signals, interference signals, and background noise in the non-underdetermined case, which is widely used in audio signal processing [5], mechanical engineering [6], and biomedical diagnosis [7–9]. A typical ICA optimization algorithm is the FastICA algorithm [10]. It should be pointed out that ICA is not suitable for underdetermined cases. For underdetermined cases, we can adopt sparse analysis [11–14], deconvolution [15, 16], and other methods. This paper only considers non-underdetermined cases.

Although the ICA method can separate the mixed signals to some extent, the signal sorting order separated by ICA is only related to the non-Gaussian of the source signal [2], so we cannot directly decide which one is the target signal, the background signal or the interference signal [4], while we are only interested in the target signal among the multiple separated signals.

In many practical applications, some characteristics of the target signal, such as the carrier frequency, modulation mode, and other prior information are known, which can be used for target signal extraction. If there is a frequency aliasing between the signals, the signal cannot be separated by the traditional filtering method. In this case, the constrained ICA (cICA) algorithm [17–19], incorporating prior information, can be used to extract the target signal [20, 21]. The cICA is also called ICA with reference (ICA-R) [22].

However, in the process of optimization for the cICA algorithm, we need to set threshold parameters to distinguish target signals from other signals, which increases computation

complexity and storage space and converges slowly. In some cases, the cICA algorithm cannot be converged [22–25].

Recently, Shi et al. proposed a new model of ICA with reference signal (ICA-R), where an adaptive weighted summation method is introduced to solve the multiobjective optimization problem with a new fixed-point learning algorithm [26, 27]. This method solves the threshold setting problem of cICA and effectively overcomes the problem of false extraction but faces the problem of determining the weight parameter.

Compared with the cICA algorithm or ICA-R, the proposed enhanced ICA with reference (EICA-R) directly contains the prior information into the ICA framework. By combining with the negative entropy contrast function and target signal distance metric function, the EICA-R establishes a unified cost function so that the constrained optimization problem is transformed into an unconstrained optimization to overcome the problem of the threshold setting problem of distance metric function for cICA.

In the enhanced ICA with reference (EICA-R) proposed in this paper, a priori information is directly contained in the ICA framework combined with the negative entropy contrast function and target signal distance metric function.

The EICA-R puts forward four kinds of cost function to convert the constrained optimization problem into unconstrained optimization problem. By deductive analysis of the similarity of the four cost functions, EICA-R establishes a unified optimization model, in which the model weight parameter is determined to meet four kinds of cost function at the same time. It not only overcomes the difficulty of setting the threshold for distance measurement function but also solves the difficulty of setting weight parameter.

In practice, the reference signal can be obtained in advance. Under the counter condition, the interference signal is not completely consistent with the target signal in frequency and may only overlap partially. Even if it is completely in the same frequency, the modulation mode of target signal and interference signal will be different. Moreover, interference signals are usually strong noises or direct background music and other unrelated signals, which are significantly different from target signals. In addition, the transmission time and mode of target signals have certain rules, while interference signals generally lack such rules. In general, continuous interference is adopted, or the same frequency interference is sent after the detection of target signals, which has obvious lag in time. We can predict in advance the precise frequency, modulation mode, and even the law of signal transmission of the target transmitter, which can be used as the basis for designing reference signals. Accordingly, interference signal does not have these characteristics.

Of course, the reference signal we designed is only an approximate version of the "expected" reference signal, but this does not affect the validity of the results. Because the reference signal is not required to be infinitely close to the actual target signal, only the distance measurement function with the target signal is the minimum. Since the reference signal is designed based on some features of the target signal, it is obvious that its distance measurement function with the target signal is smaller than that with other interference signals.

The research in this paper focuses on target signal extraction mainly targeted at non-underdetermined system. In practice, some hybrid systems are underdetermined. In terms of the underdetermined system, scholars such as Woo et al. have conducted some fruitful researches [28–30]. It is one of our next research priorities that standing on the shoulders of giants and carrying out the rapid extraction of targets under indeterminate circumstances.

The rest of this paper is organized as follows. In Section 2, we summarize the mixed signal separation model and analyze the cICA algorithm. In Section 3, we propose the EICA-R algorithm, establishing and solving and the cost function of unconstrained optimization. In Section 4, we carry out the experiment and show a series of numerical results of the EICA-R algorithm on the monosyllabic frequency modulation signal to verify the extraction effect. Section 5 is the conclusion.

2. Mixed Signal Separation and cICA

2.1. Mixed Signal Separation Model. The M-dim ensional observation signals are produced by mixing the N-dimensional sources. It may be assumed that the mixture of signals is a linear mixture. Suppose the unknown source sources are $\mathbf{s} = [s_1, s_2, \ldots, s_N]^{\mathrm{T}}$; the observed signals are $\mathbf{x} = [x_1, x_2, \ldots, x_M]^{\mathrm{T}}$; and the mixed matrix $\mathbf{A}$ is the $M \times N$ mixing matrix. Thus, the signal mixing model can be obtained as shown in the following equation:

$$\mathbf{x} = \mathbf{A}\mathbf{s}. \tag{1}$$

The signal separation model can simply be described as follows: for the observed signal $\mathbf{x} = [x_1, x_2, ..., x_M]^{\mathrm{T}}$, we can solve a $M \times N$ dimension separation matrix $\mathbf{W}$ by means of the optimization method to get the separated signal after separation:

$$\mathbf{y} = \mathbf{W}\mathbf{x}. \tag{2}$$

In order to reduce the computation in the iteration process, we need to remove the correlation between the observed signals by whitening the data with $\mathbf{V}$ before the iteration. The observation signal after albinism $\widetilde{\mathbf{x}} = \mathbf{V}\mathbf{x}$. So the separation model is changed into

$$\mathbf{y} = \mathbf{W}\widetilde{\mathbf{x}}. \tag{3}$$

where $\mathbf{y}$ are the estimated signals for the N-dimensional sources $\mathbf{s}$. It is impossible to determine which signal is the target signal y^* from $\mathbf{y}$.

2.2. Constrained ICA and ICA with Reference. It is assumed that the target signal is y^* and the corresponding separation vector is $\mathbf{w}^*$, so that the target signal y^* is

$$y^* = \mathbf{w}^{*\mathrm{T}}\widetilde{\mathbf{x}}. \tag{4}$$

Based on the prior information of the target signal, the reference signal r is designed. In order to characterize the

proximity between each separation signal y and reference signal r, the distance metric function $\varepsilon(y,r)$ between the separation signal and the reference signal is defined as follows:

$$\varepsilon(y,r) = E\left\{(y-r)^2\right\}. \tag{5}$$

As a result, the distance between the target signal y^* and the reference signal r is always minimal for any separation signal:

$$\varepsilon(y^*,r) < \varepsilon(y_{\text{else}},r). \tag{6}$$

where y_{else} is any source signal outside the target signal.

For equation (6), in order to fully separate the different homologous signals, it is necessary to fully excavate their statistical independence. The FastICA algorithm based on the maximum negative entropy can separate the independent sources with a search direction of the maximum negative entropy. In the process of separation, when the non-Gauss measure reaches the maximum, the separation of the independent components has been completed.

It is very difficult to calculate the negative entropy, so the nonquadratic function is often used to approximate the negative entropy [10]:

$$J(y) \approx \left\{E\{G(y)\} - E\{G(v)\}\right\}^2. \tag{7}$$

where v is a random variable with the standard Gauss distribution and $G(y)$ can be shown as follows:

$$G(y) = \frac{1}{a}\log\cosh(ay). \tag{8}$$

Accordingly, $g(y) = G'(y) = \tanh(ay)$. As a result, the ICA algorithm can be expressed as

$$\begin{aligned} &\max J(y), \\ &\text{s.t. } y = \mathbf{w}^{\mathrm{T}}\widetilde{\mathbf{x}}, \\ &\widetilde{\mathbf{x}} = \mathbf{V}\mathbf{x}. \end{aligned} \tag{9}$$

To extract the target signal y^* from the separation signals, we only need to get the smallest $\varepsilon(y^*,r)$ through iteration of $\varepsilon(y,r)$. From equation (6), the distance metric function between the target signal and the reference signal is always less than any other road vector. Therefore, there must be a suitable threshold parameter ξ to satisfy

$$\begin{cases} \varepsilon(y^*,r) \le \xi, \\ \varepsilon(y_{\text{else}},r) > \xi. \end{cases} \tag{10}$$

The cICA algorithm makes use of maximization negative entropy method to solve the target signal y^* and the separation vector $\mathbf{w}^*$ with the negative entropy function as the cost function and the distance metric function as the constrained condition:

$$\begin{aligned} &\langle y^*, \mathbf{w}^* \rangle = \max J(y), \\ &\text{s.t. } y = \mathbf{w}^{\mathrm{T}}\widetilde{\mathbf{x}}, \\ &\varepsilon(y,r) \le \xi. \end{aligned} \tag{11}$$

It is difficult to set the threshold parameter ξ in equation (11) for the existing cICA algorithm. When it is set too small, no separation vector conforms to the conditions; when it is too large, multiple separation vectors conform to the conditions. We abandon the method of setting threshold parameters and solve the problem directly from $\min \varepsilon(y,r)$.

To solve the problem of setting threshold parameters ξ, some improved ICA-R algorithms are formulated [22, 26, 27]. This method solves the threshold setting problem of cICA and effectively overcomes the problem of false extraction but faces the problem of the weight parameter. For instance, Li used two cost functions at the same time to make two optimization operations, in which a rough pretreatment was carried out first, and then a fine post-processing was carried out [22]. What this paper considers is to combine two kinds of functions into a cost function, which can be optimized once. In this way, four kinds of cost functions are produced, among which the problem of parameter setting is involved. By combining the four kinds, the problem of parameter setting is effectively solved.

3. Enhanced ICA with Reference

3.1. EICA-R Cost Function. With the combination of (9) and (10), the target signal y^* needs to meet two optimization problems at the same time:

$$\begin{cases} \max J(y), \\ \min \varepsilon(y,r). \end{cases} \tag{12}$$

In order to describe the two optimization problems in a unified way, the maximization and minimization can be transformed into each other. $\max J(y)$ can be converted to $\min 1/(J(y)+1)$ or $\min -J(y)$; similarly, $\min \varepsilon(y,r)$ can be converted to $\max 1/(\varepsilon(y,r)+1)$ or $\max -\varepsilon(y,r)$. So we can describe the problem of target signal y^* extraction in two directions and get four EICA-R solutions.

Direction 1: combining the distance metric function and the negative entropy contrast function, we reduce the constrained conditions and establish two forms of cost functions $F(\mathbf{w})$, according to the different transformation forms of $\max J(y)$:

$$F_1(\mathbf{w}) = \frac{\varepsilon(y,r)}{(J(y)+1)}, \tag{13}$$

$$F_2(\mathbf{w}) = \mu\varepsilon(y,r) - \lambda J(y), \tag{14}$$

where μ and λ are the positive scaling factors. The corresponding EICA-R schemes are shown as follows:

$$\mathbf{w}^* = \min \quad F_1(\mathbf{w}), \tag{15}$$

$$\begin{aligned} \mathbf{w}^* = \min \quad & F_2(\mathbf{w}), \\ \text{s.t.} \quad & \lambda, \mu > 0. \end{aligned} \tag{16}$$

Since the selection of μ and λ has a great impact on As, $F_2(w)$ in equation (14) is related to the selection of appropriate parameters μ and λ, and the optimization result of equation (16) depends on μ and λ. This problem does not exist in equation (15), whose optimization result is reliable. Therefore, μ and λ need to be set appropriately so that the

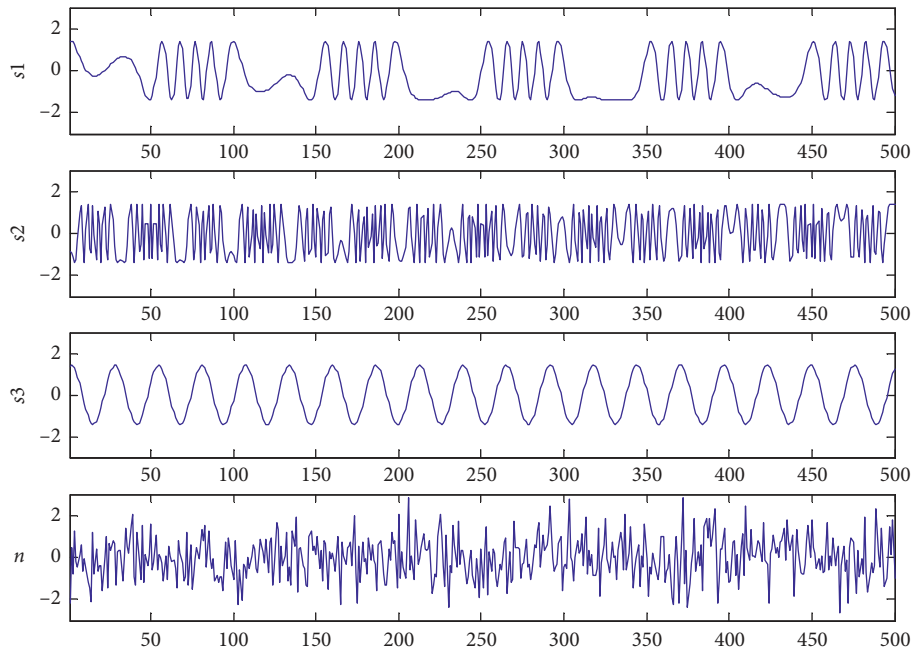

Figure 1: Waveform diagram of source signals.

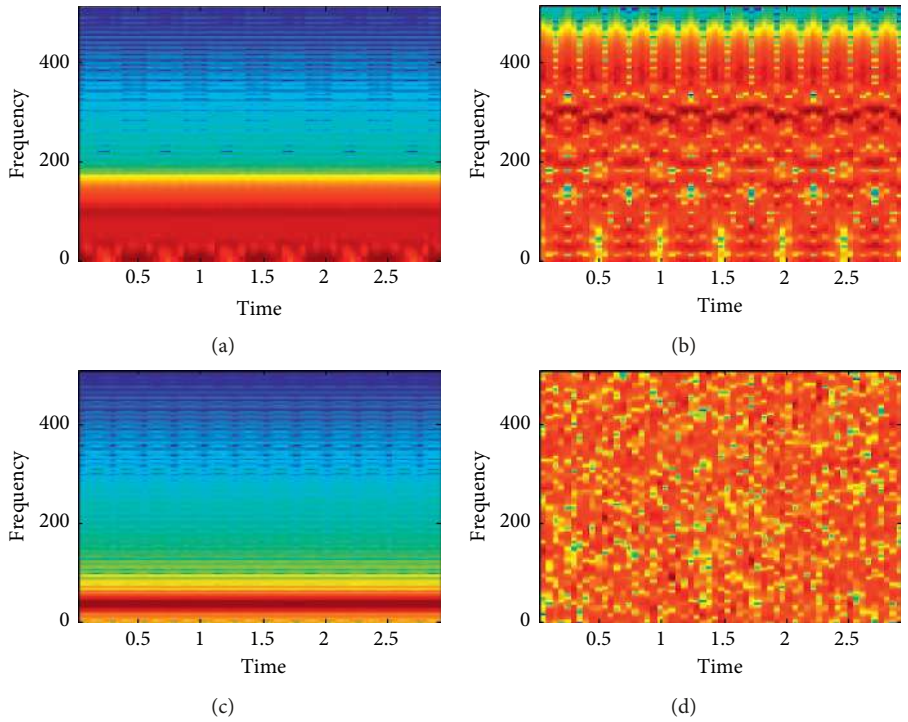

Figure 2: Spectra of source signals. (a) s_1. (b) s_2. (c) s_3. (d) n.

final optimization result of equation (16) is consistent with equation (15).

Direction 2: combining the distance metric function and the negative entropy contrast function, we reduce the constrained conditions and establish two forms of cost functions $F(\mathbf{w})$, according to the different transformation forms of $\min \varepsilon(y, r)$:

$$F_3(\mathbf{w}) = \frac{J(y)}{(\varepsilon(y, r) + 1)}, \tag{17}$$

$$F_4(\mathbf{w}) = \lambda J(y) - \mu\varepsilon(y, r), \tag{18}$$

where μ and λ are also arbitrary positive scaling factors. The cost function in equation (17) and the cost function in

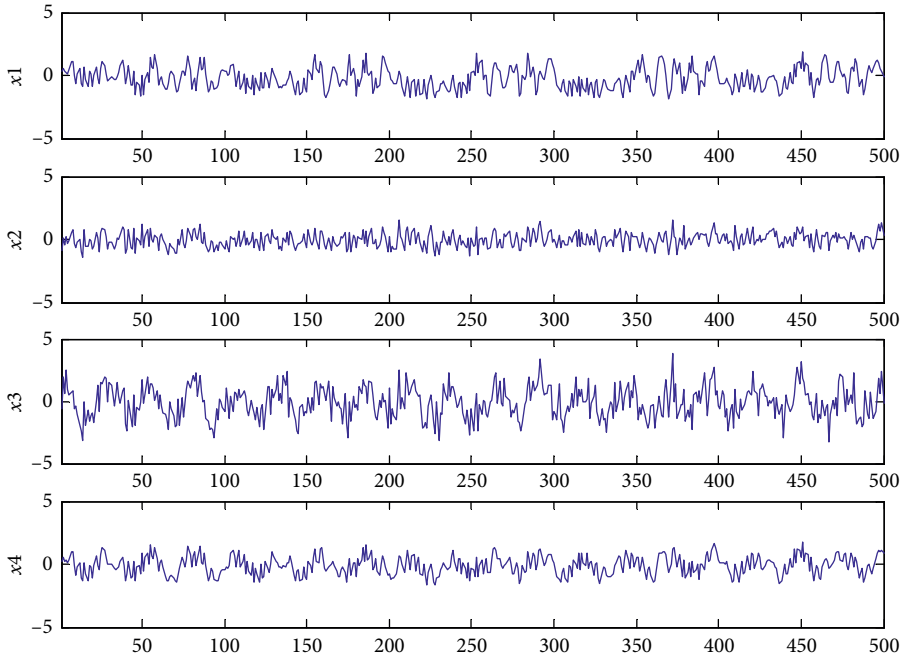

Figure 3: Waveform diagram of mixed signals.

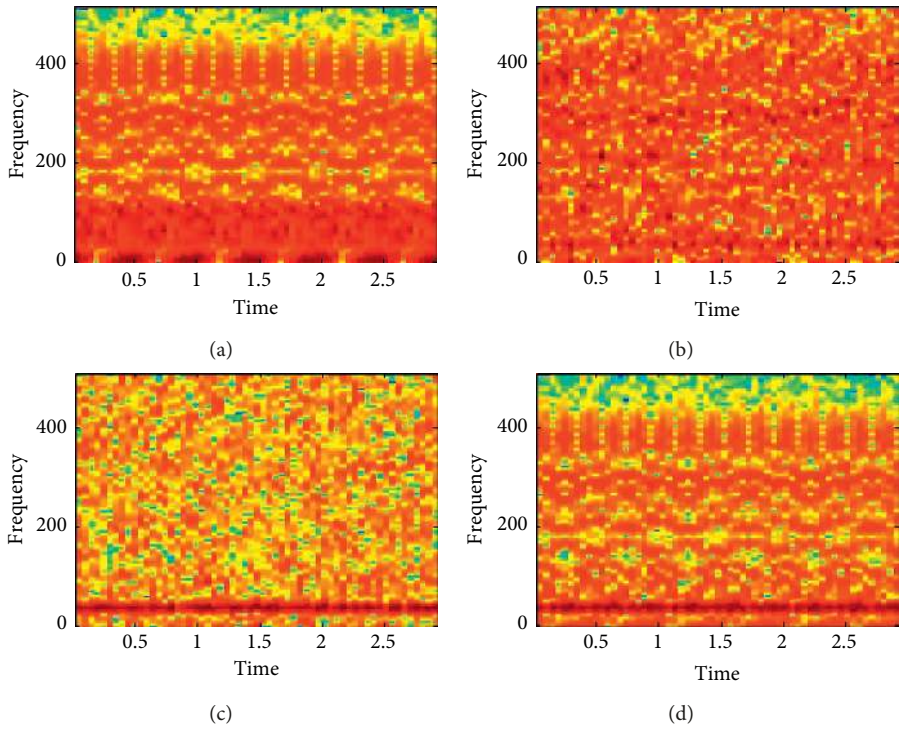

Figure 4: Spectra of mixed signals. (a) x_1. (b) x_2. (c) x_3. (d) x_4.

equation (13) are reciprocal relations, while the cost function in equation (18) is positive and negative with the cost function in equation (14). Then, the corresponding EICA-R scheme is shown in the following expressions:

$$\mathbf{w}^* = \max \quad F_3(\mathbf{w}), \tag{19}$$

$$\mathbf{w}^* = \max \quad F_4(\mathbf{w}), \quad \text{s.t.} \quad \lambda, \mu > 0. \tag{20}$$

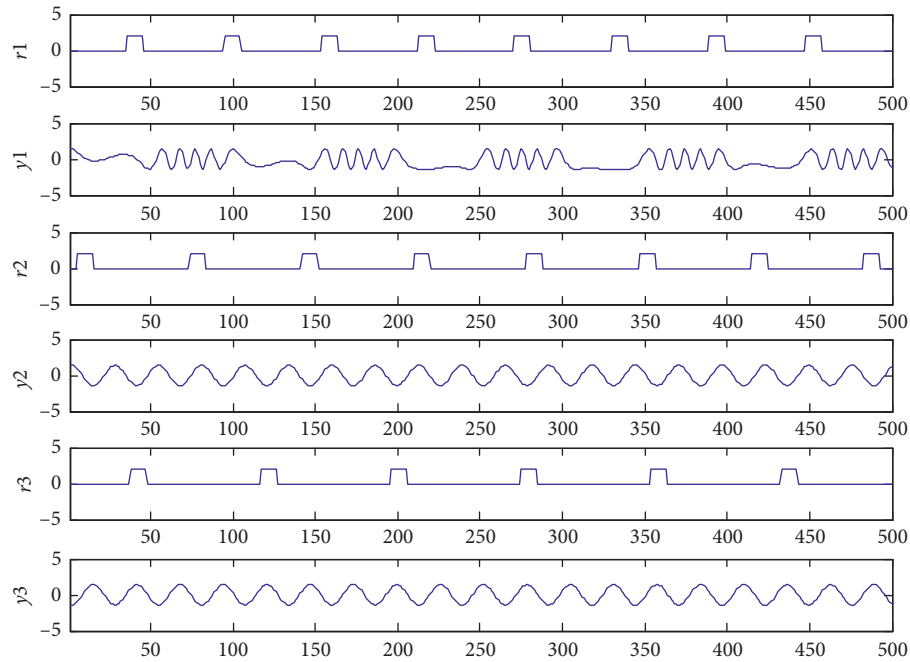

Figure 5: The extraction effect 1 of the cICA method.

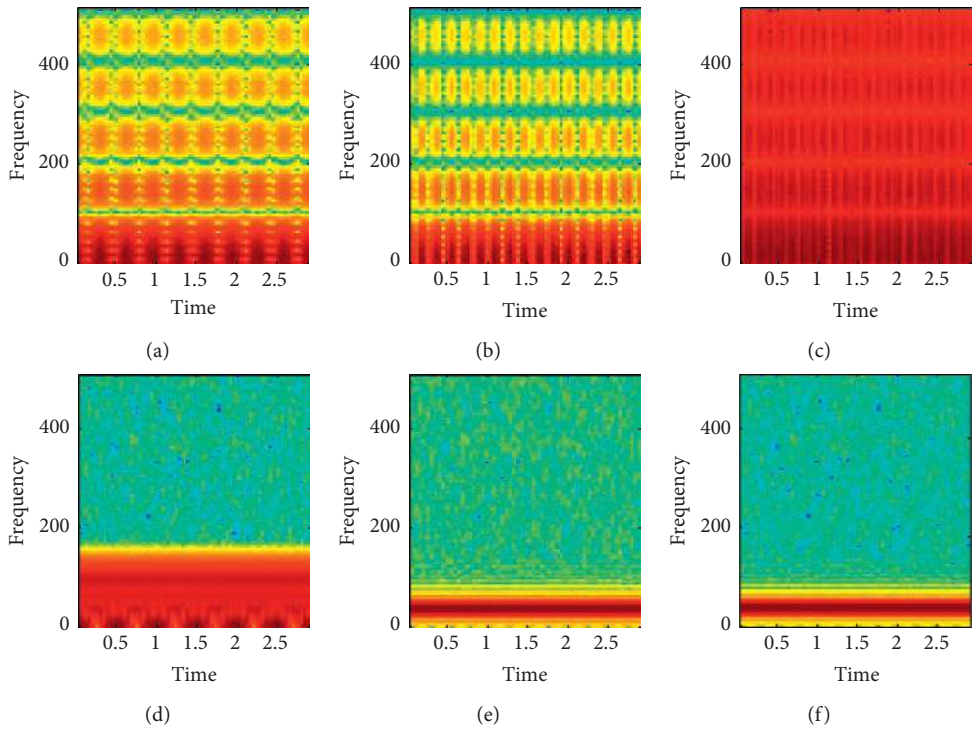

Figure 6: Spectra 1 of the cICA method. (a) r_1. (b) r_2. (c) r_3. (d) y_1. (e) y_2. (f) y_3.

The scheme of (19) and (20) is corresponding to the scheme of (15) and (16). It also faces the problem of division operation or scaling factor setting iteration. Similarly, μ and λ need to be set appropriately so that the final optimization result of equation (20) is consistent with that of equation (19).

According to the comprehensive analysis of equations (12)–(20), the optimization results of equations (15) and (19) are definite and reliable. The four equations combine the two cost functions according to four different combinations, so it is reasonable to produce four optimization algorithms.

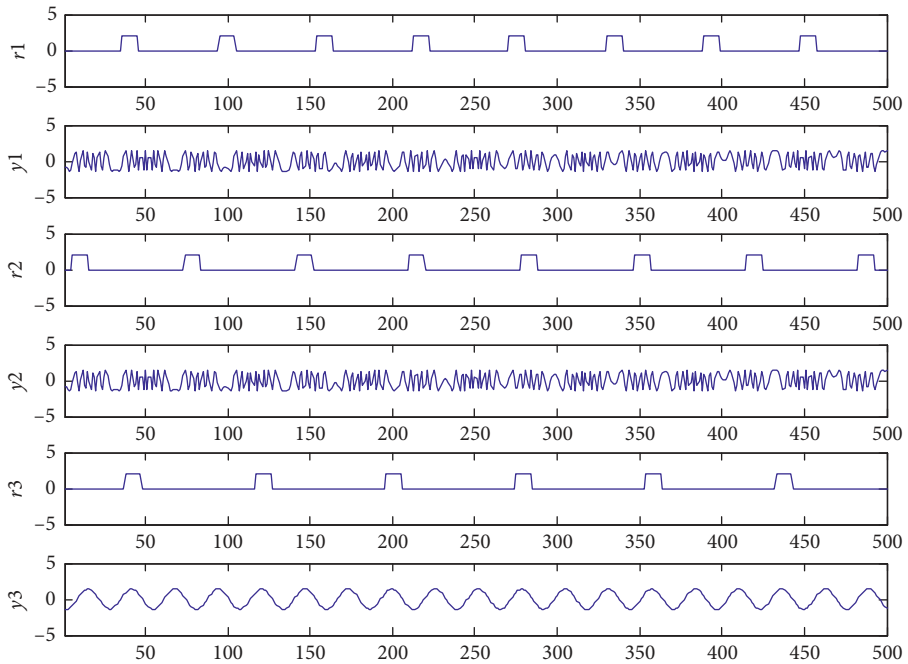

Figure 7: The extraction effect 2 of the cICA method.

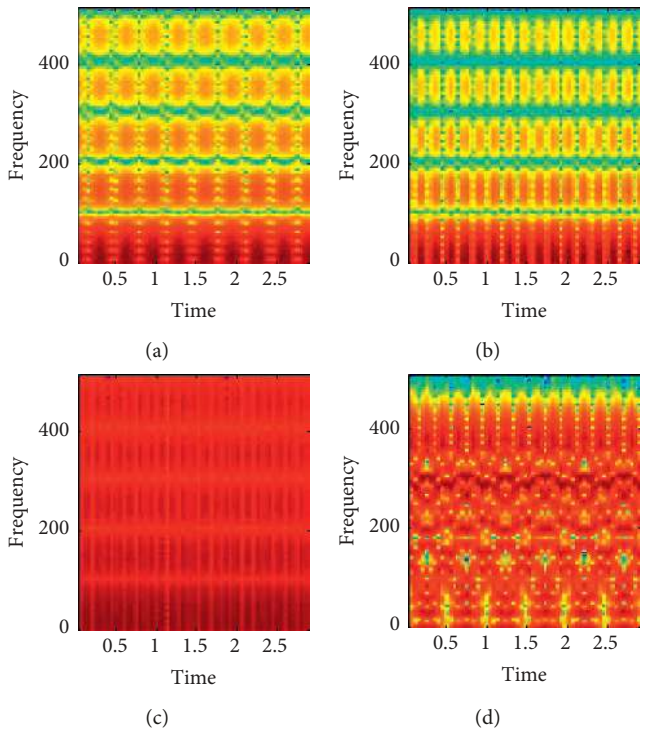

Figure 8: Continued.

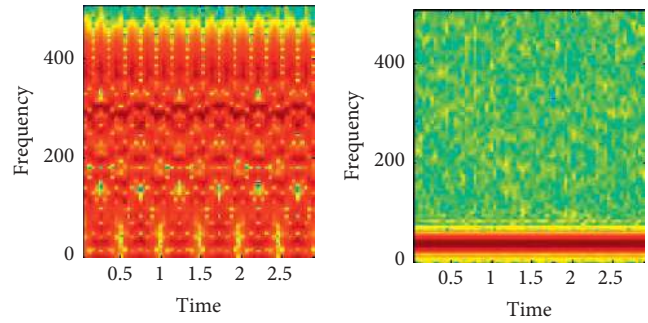

Figure 8: Spectra 2 of the cICA method. (a) r_1. (b) r_2. (c) r_3. (d) y_1. (e) y_2. (f) y_3.

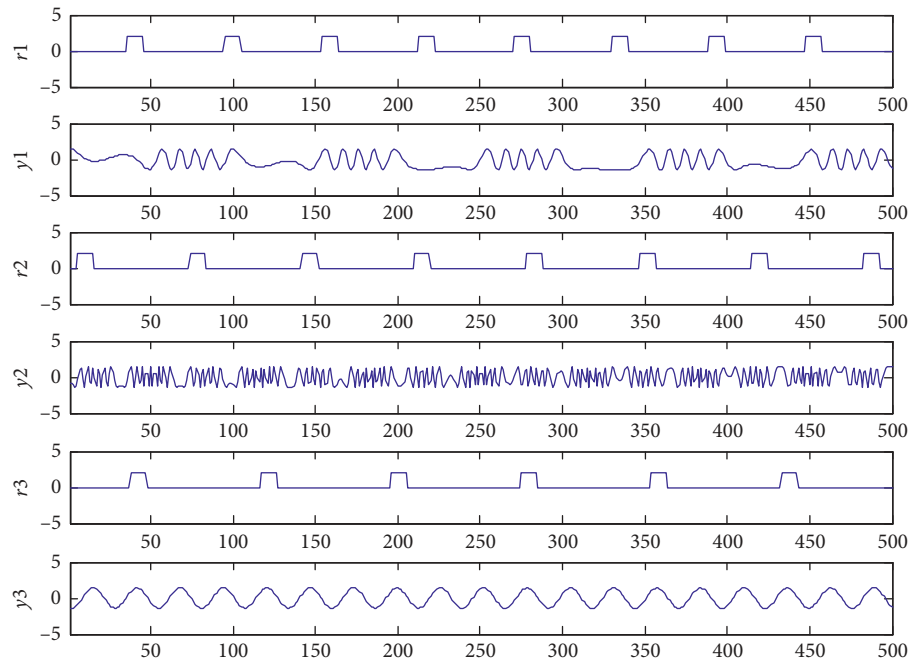

Figure 9: The extraction effect of the EICA-R method.

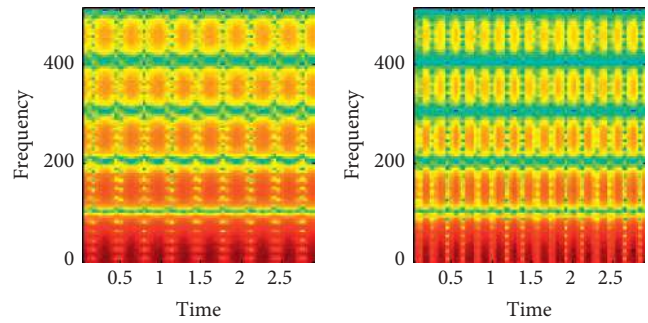

Figure 10: Continued.

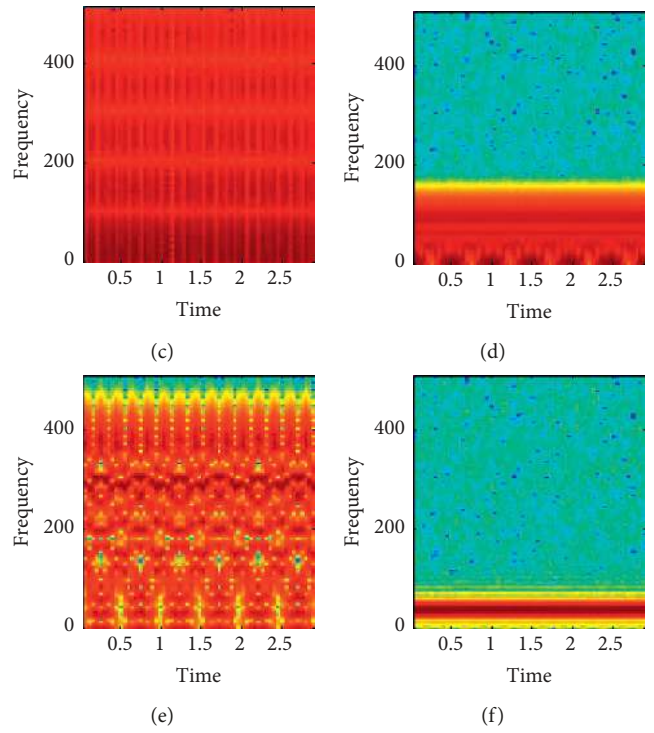

Figure 10: Spectra of the EICA-R method. (a) r_1. (b) r_2. (c) r_3. (d) y_1. (e) y_2. (f) y_3.

Now, we will try to find out the common features of equations (15), (16), (19), and (20).

Theorem 1. *The gradient of the cost function for the four EICA-R schemes $F_1(\mathbf{w})$, $F_2(\mathbf{w})$, $F_3(\mathbf{w})$, and $F_4(\mathbf{w})$ can be expressed in a similar form.*

Proof. the gradient of the cost function for $F_1(\mathbf{w})$ and $F_2(\mathbf{w})$ is shown as follows:

$$\begin{cases} \nabla F_1(\mathbf{w}) = \dfrac{1}{(J(y)+1)^2}\left((J(y)+1)\dfrac{\partial \varepsilon(y,r)}{\partial \mathbf{w}} - \varepsilon(y,r)\dfrac{\partial J(y)}{\partial \mathbf{w}}\right), \\ \nabla F_2(\mathbf{w}) = \mu\dfrac{\partial \varepsilon(y,r)}{\partial \mathbf{w}} - \lambda\dfrac{\partial J(y)}{\partial \mathbf{w}}. \end{cases} \tag{21}$$

They can be uniformly expressed as

$$\nabla F(\mathbf{w}) = \alpha\frac{\partial \varepsilon(y,r)}{\partial \mathbf{w}} - \beta\frac{\partial J(y)}{\partial \mathbf{w}}, \quad \alpha > 0, \beta > 0. \tag{22}$$

The gradient of the cost function for $F_3(\mathbf{w})$ and $F_4(\mathbf{w})$ is shown as follows:

$$\begin{cases} \nabla F_3(\mathbf{w}) = \dfrac{1}{(\varepsilon(y,r)+1)^2}\left((\varepsilon(y,r)+1)\dfrac{\partial J(y)}{\partial \mathbf{w}} - J(y)\dfrac{\partial \varepsilon(y,r)}{\partial \mathbf{w}}\right), \\ \nabla F_4(\mathbf{w}) = -\mu\dfrac{\partial \varepsilon(y,r)}{\partial \mathbf{w}} + \lambda\dfrac{\partial J(y)}{\partial \mathbf{w}}. \end{cases} \tag{23}$$

They can be uniformly expressed as

$$\nabla F(\mathbf{w}) = \alpha\frac{\partial \varepsilon(y,r)}{\partial \mathbf{w}} - \beta\frac{\partial J(y)}{\partial \mathbf{w}}, \quad \alpha < 0, \beta < 0. \tag{24}$$

So they can be expressed in a similar form:

$$\nabla F(\mathbf{w}) = \alpha\frac{\partial \varepsilon(y,r)}{\partial \mathbf{w}} - \beta\frac{\partial J(y)}{\partial \mathbf{w}}, \quad \alpha\beta > 0. \tag{25}$$

It can be obtained by using Theorem 1 that we can take a particular $F(\mathbf{w}) = \varepsilon(y,r)/(J(y)+1)$ as the cost function that is more certain. Therefore, the new description of EICA-R is shown in the following equation:

$$\mathbf{w}^* = \min F(\mathbf{w}), \tag{26}$$

where $F(\mathbf{w}) = \varepsilon(y,r)/(J(y)+1)$, $\varepsilon(y,r)$, and $J(y)$ are the distance metric functions and negative entropy contrast functions, respectively. □

3.2. Optimal Solution for Cost Functions. The gradient of $F(\mathbf{w})$ in equation (26) is expressed as follows:

$$\nabla F(\mathbf{w}) = \alpha\frac{\partial \varepsilon(y,r)}{\partial \mathbf{w}} - \beta\frac{\partial J(y)}{\partial \mathbf{w}}, \tag{27}$$

where $\alpha = 1/(J(y)+1)$ and $\beta = \varepsilon(y,r)/(J(y)+1)^2$. Define $\rho = E\{G(y)\} - E\{G(v)\}$ and g as the derivative of G. Since $y = \mathbf{w}^{\mathrm{T}}\tilde{\mathbf{x}}$, we get

$$\frac{\partial J(y)}{\partial \mathbf{w}} = 2\rho E\left\{\tilde{\mathbf{x}}g\left(\mathbf{w}^{\mathrm{T}}\tilde{\mathbf{x}}\right)\right\}. \tag{28}$$

For $\varepsilon(y,r) = E\left\{(y-r)^2\right\}$, we get

Input: The observation signal $\mathbf{x}$, the number of signal sources N, the reference signal r, the difference terminates $\eta(\eta \ll 1)$ of distance metric errors.
Output: The target signal y^*, separation vector $\mathbf{w}^*$.
Step 1: Preprocessing: whiten the observational signal $\tilde{\mathbf{x}} = \mathbf{V}\mathbf{x}$, in which $\mathbf{V}$ is obtained by using equation (3).
Step 2: Initialize:
Step 2.1: Determines the initial separation vector $\mathbf{w}^{(0)}$ with a unit norm.
Step 2.2: Determines the initial estimation signal $y^{(0)} \longleftarrow (\mathbf{w}^{(0)})^{\mathrm{T}}\tilde{\mathbf{x}}$ and the initial distance metric error $\varepsilon(y^{(0)}, r) \longleftarrow (y^{(0)} - r)^2$
Step 2.3: Determine the initial parameters: $\rho^{(0)} = E\{G(y^{(0)})\} - E\{G(v)\}$, $\alpha^{(0)} = 1/J(y^{(0)}) + 1$, $\beta^{(0)} = \varepsilon(y^{(0)}, r)/(J(y^{(0)}) + 1)^2$, $k \longleftarrow 1$.
Step 3: Iterations:
Step 3.1: According to equation (31), update $\mathbf{w}$, get $\mathbf{w}^{(k)}$. $\mathbf{w}^{(k)} \longleftarrow \mathbf{w}^{(k-1)} - 2\alpha^{(k-1)}(y^{(k-1)} - r)\tilde{\mathbf{x}} + 2\beta^{(k-1)}\rho^{(k-1)}g(y^{(k-1)})\tilde{\mathbf{x}}$.
Step 3.2: Normalize $\mathbf{w}^{(k)}$: $\mathbf{w}^{(k)} \longleftarrow \mathbf{w}^{(k)}/\|\mathbf{w}^{(k)}\|$.
Step 3.3: Update y and distance metric error: $y^{(k)} \longleftarrow (\mathbf{w}^{(k)})^{\mathrm{T}}\tilde{x}$, $\varepsilon(y^{(k)}, r) \longleftarrow (y^{(k)} - r)^2$.
Step 3.4: Update the parameters ρ, α, and β. $\rho^{(k)} = E\{G(y^{(k)})\} - E\{G(v)\}$, $\alpha^{(k)} = 1/(J(y^{(k)}) + 1)$, $\beta^{(k)} = \varepsilon(y^{(k)}, r)/(J(y^{(k)}) + 1)^2$.
Step 3.6: Update the difference ς between the distance metric errors for the iterative $\varsigma^{(k)} \longleftarrow \varepsilon(y^{(k)}, r) - \varepsilon(y^{(k-1)}, r)$.
Step 3.7: Compare ς with η, if $\varsigma^{(k)} \le \eta$, then stop iterating; otherwise, $k \longleftarrow k + 1$, go to step 3.1 to continue the iteration.
Step 4: Output results: $\mathbf{w}^* = \mathbf{w}^{(k)}$, $y^* = y^{(k)}$.

Algorithm 1: Iterative implementation process for $\mathbf{w}^*$ and y^*.

Table 1: The average SNR (dB) of the 1000 experiments.

The separate signal	FastICA	cICA	EICA-R
y_1	39.2	29.9	34.0
y_2	38.4	28.2	34.5
y_3	38.9	27.1	37.3

Table 2: The average run time(s) of the 1000 experiments.

The separate signal	FastICA	cICA	EICA-R
y_1		0.176	0.152
y_2	0.328	0.165	0.146
y_3		0.181	0.163

$$\frac{\partial \varepsilon(y, r)}{\partial \mathbf{w}} = 2E\{(y - r)\}\tilde{\mathbf{x}}. \tag{29}$$

From equations (27)–(29), we can obtain

$$\nabla F(\mathbf{w}) = 2\alpha E\{(y - r)\}\tilde{\mathbf{x}} - 2\beta\rho E\{\tilde{\mathbf{x}}g(\mathbf{w}^{\mathrm{T}}\tilde{\mathbf{x}})\}. \tag{30}$$

Thus, the gradient-based learning algorithm is shown in the following equation:

$$\mathbf{w} \longleftarrow \mathbf{w} - 2\alpha E\{(y - r)\}\tilde{\mathbf{x}} + 2\beta\rho E\{\tilde{\mathbf{x}}g(\mathbf{w}^{\mathrm{T}}\tilde{\mathbf{x}})\}, \tag{31}$$

where $g(\mathbf{w}^{\mathrm{T}}\tilde{\mathbf{x}}) = \tanh(a\mathbf{w}^{\mathrm{T}}\tilde{\mathbf{x}})$. The corresponding iterative algorithm process is shown in Algorithm 1.

4. Simulation Experiment and Performance Analysis

4.1. Experimental Signal. In the experiment, 10 groups of analog signals with different systems were selected. A total of 1000 experiments were conducted. One group of signals, in which the frequency of each signal was close to each other, is shown as follows: the source signals s_1 and s_2 are the single tone FM-modulated signals, while the source signal s_3 is the carrier signal. For instance, a set of experimental signals is as follows:

$$\begin{aligned} s_1 &= \sin\left(2\pi F_1 T_s k + 6\cos\left(2\pi f_1 T_s k\right)\right), \\ s_2 &= \cos\left(2\pi F_2 T_s k + 24\cos\left(2\pi f_2 T_s k\right)\right), \\ s_3 &= \cos\left(2\pi F_3 T_s k + 2\right). \end{aligned} \tag{32}$$

For the convenience of displaying signals, we take the frequency as $F_1 = 510\,\mathrm{Hz}$, $F_2 = 440\,\mathrm{Hz}$, $F_3 = 380\,\mathrm{Hz}$, $f_1 = 100\,\mathrm{Hz}$, and $f_2 = 150\,\mathrm{Hz}$. These signals overlap each other in the frequency domain and cannot be separated and extracted by filtering. In addition, a random white Gaussian noise signal is produced as s_4. As a result, the 4 source signals and corresponding spectra are shown in Figures 1 and 2.

An $M \times N$ ($M = N = 4$) mixed matrix $A_{4\times4}$ is generated randomly to mix the source signals, and then the mixed signals and corresponding spectra are shown in Figures 3 and 4.

For the target signal we need, this prior information is desirable. For example, in the case of 4×4 mixture, we need to analyze the number of the target signals. Take communication signals as an example, one of which is our normal communication signals and the other is antijamming signals and unintentional jamming signals. Then, only our normal communication signals are our target signals. The prior information of transmitter signal of our communication object can be known, which is sufficient to extract the target signal we need.

The reference signals should carry the prior information of the expected source signals with non-Gauss characteristic. There are many kinds of reference signal design, and the most typical method is the pulse method. We select the pulse signals with the same frequency as the source signals as the reference signals.

4.2. Experimental Result. In practice, for example, only one of the 4 signals need to be extracted, which means that only one signal is needed to extract the source signal.

In the simulation experiment, in order to compare the performance with cICA, we designed the reference signal for each signal and extracted each signal.

In order to compare the separation effect conveniently, we carry out the separation experiment by means of the EICA-R method proposed in this paper and the cICA method.

Firstly, we use the method of cICA to carry out simulation experiments [27]. In general, in cICA we do not know the correct threshold parameter ξ. In order to ensure that the solution of the required independent components is in the feasible region of the inequality, the initial value of $\xi^{(0)}$ is given to a larger value so that the feasible region is large enough. For the normalized signal y_{else} and r, $\xi < \varepsilon(y_{\text{else}}, r) < 1$. If the initial value $\xi^{(0)}$ is set as 1, all independent components in the possible region can be obtained; that is, all target signals can be extracted simultaneously. In this case, the range of ξ needs to be narrowed repeatedly until no signal is extracted when $\xi^{(k)}$. Taking $\xi^{(k-1)}$ as the threshold ξ, then 1000 experiments were repeated.

According to the experiment using the cICA method, different reference signals appear many times and the same target signal is extracted. For 1000 experiments with the cICA method, about 1/10 was erroneously extracted. Some results of these experiments are shown in Figures 5–8.

The key to the cICA algorithm is the setting of the threshold ξ that cannot guarantee the accuracy of the extraction signal. If the threshold is too large, there are lots of source signal vectors $\mathbf{w}^*$ satisfying the inequality, then the output of the system cannot be just interested; on the contrary, if the threshold is too small, there is no separate vector algorithm satisfying the inequality.

Then, we make use of the EICA-R method proposed to carry out the experiment. The result of 1000 times shows that no extraction error occurred, as shown in Figures 9 and 10.

The experimental results of Figures 5–10 indicate that the EICA-R method in this paper overcomes the above problems with a good extraction effect for different target signals. The separated target signal corresponds to the reference signal one by one without error extraction phenomenon.

4.3. Performance Analysis. On this basis, we continue to study and compare the separation and extraction performance. First, we study the SNR of the extracted target signal, and the SNR of each target signal extracted is as follows:

$$\text{SNR}_j = 10\log_{10}\frac{\sum_{k=1}^{3000} y_j^2(k)}{\sum_{k=1}^{3000}\left[y_j(k) - s_i(k)\right]^2}, \tag{33}$$

where s_i is the i-th source signal and y_j is a separate signal corresponding to the target signal. For the EICA-R method, y_i are in one-to-one correspondence with source signals s_i; for the cICA method, when eliminating the extraction results error, y_i are all in one-to-one correspondence with the source signals s_i. For the FastICA method, since the corresponding relationship is random, we take the form of highest SNR for each y_j. The average SNR of the 1000 independent experiments is shown as shown in Table 1.

Table 1 shows that the antinoise performance of the EICA-R method proposed in this paper is less than that of the FastICA method, but it is superior to the cICA method. This is because the EICA-R method and the cICA method all join the constraint conditions and the cumulative errors in the iterative process are also increased accordingly. The EICA-R method overcomes the error extraction of the cICA method, so the mean SNR of the EICA-R method is greater than that of the cICA method.

The corresponding run time is shown in Table 2.

Table 2 shows that the separation time of the EICA-R signal is less than that of cICA, and the time of separating all three signals is longer than that of FastICA, but the time of separating the single signal by EICA-R is less than half of that of FastICA. For the single target signal, the EICA-R separation efficiency is the highest. That is determined by the computational complexity of the respective algorithms. Tables 1 and 2 also show that this algorithm improves the separation signal quality and separation efficiency while overcoming the error extraction of the target signal. This simple example would be suffice to show that FastICA can only separate multiple sources but cannot tell which is the target signal; the cICA algorithm can extract the target signal, but there is a problem of false extraction, which is not reliable in practical application. The algorithm in this paper can not only separate the source signal but also effectively extract the target signal and overcome the problem of false extraction.

5. Conclusion

Extracting the target signal accurately from the mixed signal is one of the difficulties in the field of signal processing. Based on the existing cICA algorithms, we propose an enhanced independent component analysis with reference (ICA-R) to overcome the shortcomings of random and false extraction of separate signal sequence in the existing hybrid signal separation algorithm. By combining the negative entropy contrast function and the distance metric function of the target signal, we establish a unified cost function, which transforms the constrained optimization problem into an unconstrained optimization problem. The EICA-R algorithm proposed in this paper not only overcomes the threshold setting problem of distance measurement function but also solves the problem of weight parameter setting. Theoretical analysis and simulation results show that the proposed ICA-R algorithm outperforms the existing algorithms in extracting the target signal.

Data Availability

The data used to support the findings of this study are available from the corresponding author upon request.

Disclosure

The initial research of this paper was published in the Conference summary of the 5th International Conference on

Information Science and Control Engineering (ICISCE) in 2018.

Conflicts of Interest

The authors declare that they have no conflicts of interest.

Authors' Contributions

All the authors made theoretical and experimental verification and analysis of the content.

Acknowledgments

This paper has been supported by the National Natural Science Foundation of China (grant nos. 61602511 and 61401513).

References

[1] H. Nie, *Complex Electromagnetic Environment Effect for Electronic Information System*, National Defense Industry Press, Beijing, China, 2013.

[2] X. Yu and D. Hu, *Blind Source Separation: Theory and Applications*, John Wiley & Sons, Singapore, 2014.

[3] P. Comon, "Independent component analysis, a new concept?," *Signal Processing*, vol. 36, no. 3, pp. 287–314, 1994.

[4] A. Hyvrinen, *Independent Component Analysis*, Wiley & Sons, New York, NY, USA, 2001.

[5] E. Vincent, "Musical source separation using time-frequency source priors," *IEEE Transactions on Audio, Speech and Language Processing*, vol. 14, no. 1, pp. 91–98, 2006.

[6] Y. Guo, S. Huang, Y. Li, and G. R. Naik, "Edge effect elimination in single-mixture blind source separation," *Circuits, Systems, and Signal Processing*, vol. 32, no. 5, pp. 2317–2334, 2013.

[7] G. Pendharkar, G. R. Naik, and H. T. Nguyen, "Using blind source separation on accelerometry data to analyze and distinguish the toe walking gait from normal gait in ITW children," *Biomedical Signal Processing and Control*, vol. 13, no. 1, pp. 41–49, 2014.

[8] R. Chai, G. Naik, T. Nguyen et al., "Driver fatigue classification with independent component by entropy rate bound minimization analysis in an EEG-based system," *IEEE Journal of Biomedical & Health Informatics*, vol. 21, no. 3, pp. 715–724, 2017.

[9] G. Naik, S. Selvan, and H. Nguyen, "Single-channel EMG classification with ensemble-empirical-mode-decomposition-based ICA for diagnosing neuromuscular disorders," *IEEE Transactions on Neural Systems and Rehabilitation Engineering*, vol. 24, no. 7, pp. 734–743, 2016.

[10] A. Hyvarinen, "Fast and robust fixed-point algorithms for independent component analysis," *IEEE Transactions on Neural Networks*, vol. 10, no. 3, pp. 626–634, 1999.

[11] H. Liu, S. Liu, T. Huang et al., "Infrared spectrum blind deconvolution algorithm via learned dictionaries and sparse representation," *Applied Optics*, vol. 55, no. 10, pp. 2813–2818, 2016.

[12] Y. Chi, "Guaranteed blind sparse spikes deconvolution via lifting and convex optimization," *IEEE Journal of Selected Topics in Signal Processing*, vol. 10, no. 4, pp. 782–794, 2015.

[13] L. Wang and Y. Chi, "Blind deconvolution from multiple sparse inputs," *IEEE Signal Processing Letters*, vol. 23, no. 10, pp. 1384–1388, 2016.

[14] W. L. Woo, S. Dlay, A. Tmeme, and B. Gao, "Reverberant signal separation using optimized complex sparse nonnegative tensor deconvolution on spectral covariance matrix," *Digital Signal Processing*, vol. 83, pp. 9–23, 2018.

[15] A. Tmeme, W. L. Woo, S. Dlay, and B. Gao, "Single channel informed signal separation using artificial-stereophonic mixtures and exemplar-guided matrix factor deconvolution," *International Journal Adaptive Control and Signal Processing*, vol. 32, no. 9, pp. 1259–1281, 2018.

[16] W. L. Woo, B. Gao, A. Bouridane et al., "Unsupervised learning for monaural source separation using maximization-minimization algorithm with time-frequency deconvolution," *Sensors*, vol. 18, no. 5, p. 1371, 2018.

[17] D. Huang and J. Mi, "A new constrained independent component analysis method," *IEEE Transactions on Neural Networks*, vol. 18, no. 5, pp. 1532–1535, 2007.

[18] W. Lu and J. C. Rajapakse, "Approach and applications of constrained ICA," *IEEE Transactions on Neural Networks*, vol. 16, no. 1, pp. 203–212, 2005.

[19] J. Li, H. Zhang, and J. Zhang, "Fast adaptive BSS algorithm for independent/dependent sources," *IEEE Communications Letters*, vol. 20, no. 11, pp. 2221–2224, 2016.

[20] Z. Wang, J. Chen, G. Dong, and Y. Zhou, "Constrained independent component analysis and its application to machine fault diagnosis," *Mechanical Systems & Signal Processing*, vol. 25, no. 7, pp. 2501–2512, 2011.

[21] W. Lu, L. Liu, and Y. Li, "Adaptive multiple subtraction based on constrained independent component analysis," *SEG Technical Program Expanded Abstracts*, vol. 74, no. 1, pp. V1–V7, 2009.

[22] C. Li, G. Liao, and Y. Shen, "An improved method for independent component analysis with reference," *Digital Signal Processing*, vol. 20, no. 2, pp. 575–580, 2010.

[23] X. Tang, J. Ye, and X. Zhang, "On the convergence of ICA algorithms with weighted orthogonal constraint," *Digital Signal Processing*, vol. 28, no. 1, pp. 39–47, 2014.

[24] G. Chen, Q. Longfei, A. Zhang, and J. Han, "Improved cICA algorithm used for single channel compound fault diagnosis of rolling bearings," *Chinese Journal of Mechanical Engineering*, vol. 29, no. 1, pp. 204–211, 2016.

[25] A. Mirzal, "NMF versus ICA for blind source separation," *Advances in Data Analysis & Classification*, vol. 11, no. 1, pp. 25–48, 2017.

[26] Y. Shi, W. Zeng, N. Wang, and L. Zhao, "A new method for independent component analysis with priori information based on multi-objective optimization," *Journal of Neuroscience Methods*, vol. 283, pp. 72–82, 2017.

[27] Y. Shi, W. Zeng, X. Tang, W. Kong, and J. Yin, "An improved multi-objective optimization-based cICA method with data-driver temporal reference for group fMRI data analysis," *Medical & Biological Engineering & Computing*, vol. 56, pp. 683–694, 2018.

[28] N. Tengtrairat, W. L. Woo, S. Dlay, and B. Gao, "Online noisy single-channel blind separation by spectrum amplitude estimator and masking," *IEEE Transactions on Signal Processing*, vol. 64, no. 7, pp. 1881–1895, 2016.

[29] N. Tengtrairat, B. Gao, W. L. Woo, and S. S. Dlay, "Single-channel blind separation using pseudo-stereo mixture and complex 2-d histogram," *IEEE Transactions on Neural Networks and Learning Systems*, vol. 24, no. 11, pp. 1722–1735, 2013.

[30] P. Parathai, N. Tengtrairat, W. L. Woo, and B. Gao, "Single-channel signal separation using spectral basis correlation with sparse nonnegative tensor factorization," *Circuits, Systems and Signal Processing*, pp. 1–31, 2019.